Revista Mexicana de Astronomía y Astrofísica, 61, 224-232, (2025)

OPEN ACCESS https://doi.org/10.22201/ia.01851101p.2025.61.03.10

Spectral and Dynamical Study of 12p/Pons-Brooks

Matheus Agenor [1,2], Daniela C. Mourão [2], Luke Dones [3], Rodolfo Langhi [1,2] and Markus Kohl[4]

[1]*Observatório Astronômico, UNESP, Brasil.*
[2]*Grupo de Dinamica Orbital e Planetologia, UNESP, Brasil.*
[3]*Southwest Research Institute, SwRI, United States.*
[4]*Realschule Hauzenberg, Hauzenberg, Germany.*

Keywords: *Celestial mechanics, Comets: individual (12P/Pons-Brooks), Method: numerical, Techniques: spectroscopic*

Abstract

We present a spectral and dynamical study of the Halley-type comet 12P/Pons-Brooks (∼ 71 year period), confirming its intense cometary activity. We performed an N-body simulation, integrating its orbit for 2×10^5 years, to analyze its chaoticity and close encounters with Venus, Earth, Mars, Jupiter, and Saturn. The orbit becomes highly chaotic for $t < 20 \times 10^3$ years, with significant instabilities arising between $15 - 20 \times 10^3$ years. We calculate a Lyapunov time of ∼ 200 yr.

Resumen

Presentamos un estudio espectral y dinámico del cometa tipo Halley 12P/Pons-Brooks (cuyo período es de ∼ 71 años), confirmando una intensa actividad cometaria. Realizamos una simulación de N-cuerpos, integrando su órbita durante 2×10^5 años para analizar su caoticidad y encuentros cercanos con Venus, Tierra, Marte, Júpiter y Saturno. La órbita se vuelve altamente caótica para $t < 20 \times 10^3$ años, con inestabilidades significativas que surgen entre $15 - 20 \times 10^3$ años. Calculamos un tiempo de Lyapunov de ∼ 200 años.

Corresponding author: Matheus Agenor *E-mail address:* matheus.agenor@unesp.br
Received: April 22, 2025 **Accepted:** October 16, 2025

1. Introduction

Comets are conglomerates of rocks and ice composed mainly of volatile materials, often referred to as dirty snowballs, a term introduced by Whipple to describe his theoretical model (Whipple, 1950). Since ancient times, comets have fascinated humanity, with records in paintings, drawings, and historical documents. Observed for millennia, until the 16th century, they were generally considered omens of misfortune (Schechner, 1999; Sagan & Druyan, 2011; Newburn & Yeomans, 1982; Oates, 1986).

The study of the chemical and physical properties of comets provides significant constraints for dynamical models of Solar System formation and evolution (Gomes et al., 2005; Walsh et al., 2011; Raymond & Izidoro, 2017). Comet spectroscopy has been fundamental in understanding their composition and how they may have contributed to the formation of the Solar System and the evolution of life on Earth. For instance, the detection of complex organic molecules in comets suggests that these celestial bodies may have played a crucial role in delivering the ingredients necessary for the origin of life on Earth (Mumma et al., 1993; Irvine et al., 2000; Bockelée-Morvan et al., 2004; Mumma & Charnley, 2011). Furthermore, the analysis of comet composition can provide information about the conditions under which the Solar System formed and evolved over time (Gomes et al., 2005; Walsh et al., 2011; Cochran et al., 2012; Raymond & Izidoro, 2017).

The comae of comets have been primarily investigated through the observation of emission spectra. To study their nuclei, cometary activity must be low. Such studies allow the exploration of the formation of nuclei within the protoplanetary disk of our system, as well as their thermal processing history (Ceccarelli et al., 2022). Most of the species observed in the optical and ultraviolet wavelengths are radicals, atoms, and ions that do not sublimate directly from the nucleus but are produced in the coma through the photodissociation of parent molecules and chemical reactions (Bockelée-Morvan et al., 2004). For example, the most common reaction is the photodissociation of water molecules into hydroxyl radicals and hydrogen: $H_2O + h\nu \rightarrow H + OH$, where h is Planck's constant and ν is the frequency of the solar photon. A cometary spectrum is characterized by two components: a reddened solar spectrum reflected by dust and an emission spectrum produced by various gaseous species in the coma. Emission lines are generated through collisional or radiative excitation processes. Because cometary comae have low densities, collisions are generally negligible. Radiative processes are the most common, producing transitions between electronic, rotational, and vibrational energy levels. Electronic transitions appear in the ultraviolet range and are rarely observed, as interaction with the Sun's UV radiation tends to dissociate molecules into their radicals. Rotational and vibrational transitions are observed in the infrared and microwave ranges, and can be detected through resonance fluorescence, which is the process of absorption followed by spontaneous re-emission.

The type of detectable emission lines or bands in the spectrum varies with the selected spectral range. In the visible (3500-7500 Å), CN can be observed, with its $\Delta\nu = 0$ band near 3880 Å,

one of the strongest spectral features in comets, almost always detectable (Feldman et al., 2004). Near this peak lies the C_3 band at 3920-4100 Åand, finally, the Swan bands of C_2 $\Delta\nu = 1$ at 4500-4745 Å, $\Delta\nu = 0$ at 5000-5174 Å, and $\Delta\nu = -1$ at 5410-5640 Å. Other features include NH_2 lines scattered throughout the spectrum (Cochran & Cochran, 2002), CH (4300-12 Å), OI lines (5577, 6300, 6364 Å), and the sodium doublet (5890, 5896 Å). Results from satellite missions have provided deeper insights into the morphology and composition of comets, revealing that their nuclei are composed mainly of refractory material and volatile ices, which are considered the most primitive remnants of the original presolar nebula (Mumma & Charnley, 2011). The composition of these ices is approximately 80% water ice, followed by CO_2, CO, CH_3OH, CH_4 H_2S, and NH_3. Among the studied comet population, H_2O, CO, CO_2, CH_4 C_2H_6, CH_3OH, H_2CO, NH_3, HNC, CH_3CN, and H_2S are among the most abundant molecules (Bockelée-Morvan & Biver, 2017).

In this work, we present a study of the spectrum and orbital dynamics of comet 12P/Pons-Brooks, discovered at the Marseille Observatory in July 1812 by Jean-Louis Pons and recovered in 1883 by William Robert Brooks (Yeomans, 1986), by Elizabeth Roemer in 1953, and by Ye et al. in 2020 (Ye et al., 2020). This comet has an orbital period of approximately 71 years and is one of the brightest known periodic comets, reaching an absolute visual brightness of approximately 5 mag at its perihelion (Meyer et al., 2020). The comet is also known for its recurrent and intense outbursts, which have been extensively documented during its recent approach to the perihelion (Jewitt & Luu, 2025). The composition and spatial distribution of its gaseous coma have been the subject of detailed spectroscopic studies (Ferellec et al., 2024), and its long-term orbital evolution has been analyzed in the context of Halley-type comet dynamics, confirming its chaotic nature (Królikowska et al., 2025).

While Ferellec et al. (2024) focused on the evolution of the coma across multiple epochs before perihelion, our work presents a spectrum obtained in a single epoch on April 6, 2024, very close to its perihelion on April 21, capturing a moment of potentially maximum activity. Furthermore, our dynamical analysis, while consistent with the findings of chaotic behavior by Królikowska et al. (2025), focuses on observing the dynamics of a significant number of clones around comet 12P to detail its short-term instability and close encounters.

The remainder of this paper is structured as follows: § 2 describes our methodology, detailing the spectral analysis (2.1) and the dynamical simulation (2.2) we performed. § 3 presents the results of the spectroscopic analysis (3.1), dynamical simulation (3.2), and Lyapunov Time and Orbital Chaos analysis. Finally, § 4 provides a discussion of our findings along with our conclusions.

2. Methodology

We approached and analyzed comet 12P/Pons-Brooks from two perspectives: an observational perspective, studying the comet's spectrum at a specific moment in its trajectory, and a theoretical perspective, simulating the comet's dynamical evolution. In this section, we present the methodology used in this study.

2.1. The Spectral Analysis

For data acquisition, a Shelyak Alpy 600 spectrometer with a slit width of 23 μm and a 600-line grating was used, alongside a ZWO ASI 071 polychromatic camera and a Skywatcher Esprit 150 APO apochromatic refractor telescope (f/7) on a Skywatcher AZ-EQ6 mount. This spectrometer was chosen for its ability to provide a good spectral resolution, enabling the identification of specific cometary emission lines. The slit was placed over the inner coma.

To calibrate the instrumental response and the λ/pix ratio, the spectrum of the A0V-type star Vega was compared with that recorded by the instrument. Using the Balmer series lines present in the spectrum of Vega, a third-order polynomial calibration curve was applied, resulting in a dispersion of approximately 2.4 Å/pix for the spectrum.

For image acquisition, the Firecapture[1] software was used, while Fitswork[2] was employed for image stacking. A total of 9 exposures of 60 s each were stacked, although the resulting spectrum remained very noisy. Spectral analysis was conducted using the RSpec[3] software. For line identification, we used the work of Walker (2017) as a reference. The observations were made in Hauzenberg, Germany, at 19:15 UTC on April 6, 2024, when the comet was located at approximately 02h 33m RA and $-19°54'$ DEC, with an apparent magnitude of ~ 4.7, positioned at 289.9° azimuth and 8.7° altitude, that is, very low in the sky.

An important aspect to consider in comet spectroscopy is the effect of atmospheric extinction, which can interfere with spectral analysis. Furthermore, several skyglow lines disturb cometary emissions. The RSpec software allows for the correction of this effect during processing. Another correction in the comet spectra is the removal of the solar contribution. Because the Sun is a highly bright and extended source, solar analogs (e.g., G2V-type stars) are typically used for this purpose (see Evangelista-Santana, 2022). However, these corrections could not be applied using RSpec in this study, causing a low elevation in the spectrum and the observation of atmospheric elements; however, this did not interfere with our study.

2.2. Dynamical Simulation Setup

We also performed a simulation to investigate the orbital dynamics of the comet. For the simulation, a reference system was established with the Sun at the center, using time in years, distance in astronomical units (AU), and mass in solar mass units. All planets were included in the system using their precise ephemerides extracted from the JPL Horizons database through the N-body integrator `REBOUND` (Rein & Liu, 2012; Rein & Spiegel, 2015). 12P/Pons-Brooks was introduced with its known orbital parameters, including the semi-major axis, eccentricity, inclination, longitude of the ascending node, argument of perihelion, and mean anomaly.

For the dynamical simulation, we created a cloud of 1000 test particles (clones) to explore the orbital evolution, considering the uncertainties in the nominal orbit. The clones were generated by varying three orbital elements: semi-major axis (a), eccentricity (e), and inclination (i). For each of these elements, a value was randomly sampled from a uniform distribution within the 1σ uncertainty interval provided by JPL Horizons (Table 1). The remaining orbital elements—longitude of the ascending node (Ω), argument of perihelion (ω), and mean anomaly (M)—were kept identical to those of the nominal orbit for all 1000 clones. The integration of the equations of motion was performed using a numerical method over a time interval of $\pm 10^5$ years, with the initial state of the system set to the date 2023-09-22 00:00 UTC.

During integration, the orbital elements of the comet were monitored, particularly the semi-major axis, eccentricity, and orbital inclination, together with the spatial coordinates relative

[1] https://www.firecapture.de/
[2] https://www.fitswork.de/
[3] https://rspec-astro.com/

Table 1. Osculating Orbital Elements of 12P/Pons-Brooks Comet[a]

Element	Value	Uncertainty (1σ)	Units Units
e	0.9545610886812381	1.1098×10^{-8}	
a	17.18488881545268	2.3125×10^{-7}	AU
q	0.7808626389081372	1.9082×10^{-7}	AU
i	74.19089780092244	4.8215×10^{-6}	deg
node	255.8552998314876	1.5858×10^{-5}	deg
peri	198.9879546650287	1.0729×10^{-5}	deg
M	357.0789668677643	2.2111×10^{-7}	deg
tp	2460421.631240357939	1.525×10^{-5}	TDB
	2024-Apr-21.13124036		
period	26020.67251140143	0.00052521	d
	71.24071871704703	1.4379×10^{-6}	y
n	0.01383515356270133	2.7926×10^{-10}	deg/d
Q	33.58891499199722	4.5198×10^{-7}	AU

[a]Reference: JPL K242/73 (heliocentric IAU76/J2000 ecliptic). Epoch 2460210.5 (2023-Sep-23.0) TDB. The columns represent: [1] orbital element, [2] value, [3] associated uncertainty, and [4] unit.

to the Sun. We sought to identify the approaches between the comet and Venus, Earth, Mars, Jupiter, and Saturn. To determine the close encounters of the comet and its particles as a function of time, we used the radius of the Hill sphere of each planet.

According to Meyer et al. (2020), the orbit of comet 12P has a chaotic behavior, preventing simulations of many thousands of years without using variational methods. In this study, we used the IAS15 method (Rein & Spiegel, 2015) to simulate the orbit of comet 12P, which offers advantages for capturing details of close interactions and chaotic behaviors on moderate timescales (a few tens of thousands of years). IAS15 is a 15th-order adaptive integrator that automatically selects its time step to maintain a predefined level of accuracy. This parameter, which controls the precision of the integrator, was not explicitly set in the simulation code; therefore, the default value of 10^{-9} was used (Rein & Spiegel, 2015). IAS15 is a good option for cases in which accuracy is critical; however, it has a higher computational cost than integrators such as Leapfrog or Runge-Kutta of order 4.

Emelyanenko (1985) finds that 12P is in a 1:6 resonance with Jupiter (he called this a 6:1 resonance). That is, it completes one orbit for every six orbits of Jupiter. Emelyanenko estimates that 12P will remain in resonance for at least another 300 orbits, or approximately 20 thousand years, assuming a purely gravitational orbit.

Table 2. Index of observed molecules[a]

Substance.	λ (Å)	Band
CN	3883	$\Delta\nu = 0$
C_2	4380	$\Delta\nu = 1$
C_2	4702	$\Delta\nu = 1$
C_2	4723	$\Delta\nu = 1$
C_2	4738	$\Delta\nu = 1$
C_2	4745	$\Delta\nu = 1$
C_2	4753	⋯
CN_2	5140	⋯
C_2	5165	$\Delta\nu = 0$
C_2	5541	$\Delta\nu = -1$
C_2	5585	$\Delta\nu = -1$
Na	5890	(D line)
Na	5896	(D line)
NH_2	5980	⋯
C_2	6122	⋯
OI	6300	⋯

[a]Col. [1] shows the substance, Col. [2] shows the wavelength in Å and Col. [3] shows the identified spectral band.

3. Results

3.1. Spectroscopic Analysis

With the extracted spectrum, calibrating the wavelength as a function of the intensity, we were able to detect CN, C_2, NH_2, the Na doublet, and OI lines. The identified emission lines and bands are shown in Figure 1 and listed in Table 2.

The detection of these significant emission bands is consistent with studies of other comets, such as those performed by Bockelée-Morvan et al. (2004) and Mumma & Charnley (2011), who also identified CN and C_2 as common components in cometary comae. A detailed analysis of the most prominent species is presented below.

Comet 12P exhibited a prominent CN line ($B^2\Sigma^+ - X^2\Sigma^+$) at 3883 Å($\Delta\nu = 0$). This feature is particularly important because cyanogen is one of the most abundant compounds in comets, indicating rich carbon and nitrogen chemistry (Munaretto et al., 2023; Aravind et al., 2024). Mura (2023) investigation showed signs of recurrent eruptions in the CN production rate of this comet, manifesting as distinct peaks corresponding to each eruption event in this same spectral region. Our spectrum corroborates the findings of Mura (2023) and Mura et al. (2024). However, we did not observe the N_2^+ line at 4238 Å.

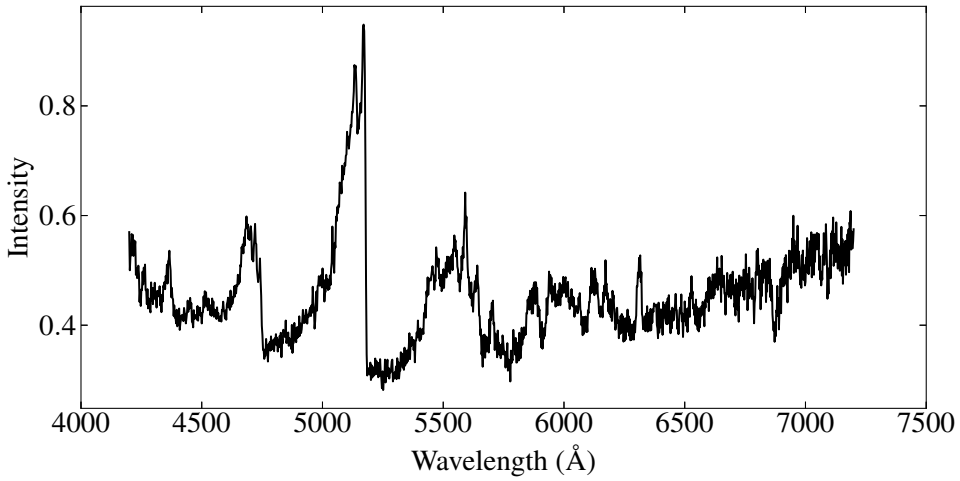

Figure 1. Spectrum of comet 12P/Pons-Brooks. The spectrum was obtained using a 600 l/mm diffraction grating. The wavelength in Angstroms and the intensity in arbitrary units.

We also observed multiple Swan bands of diatomic carbon (C_2), most notably the 5165 Åand 5585 Ålines, which are commonly found in comet spectra (de Konkoly, 1884). The presence of multiple C_2 bands suggests a diversity of vibrational states, reflecting the variable physical conditions in the comet's coma. These bands indicate the presence of diatomic carbon, which is thought to be formed by the photodissociation of more complex organic compounds, such as acetylene (C_2H_2) or ethylene (C_2H_4). This dissociation occurs under the action of solar radiation, which breaks chemical bonds and releases smaller fragments, such as C_2 and H_2. However, we cannot affirm that such a reaction occurred without studying the spectrum as a function of orbital evolution (Kohoutek & Rahe, 1976; Cambianica et al., 2021).

The NH_2 emission line at 5980 Åin the comet spectrum suggests active photochemical processes involving ammonia (NH_3). As the comet approaches the Sun, ultraviolet radiation can cause the photodissociation of ammonia molecules, breaking them into NH_2 radicals and hydrogen atoms. These NH_2 radicals emit light upon returning to the ground state, resulting in the characteristic emission line (Kawakita & Watanabe, 2002; Opitom et al., 2021). The presence of this line can thus serve as an indicator that solar radiation actively breaks down ammonia molecules present in the comet. Previous studies have identified the NH_2 line as an indicator of ammonia abundance and photochemical intensity in cometary comas (Kawakita & Watanabe, 2002; Opitom et al., 2021). The detection of this line in the spectrum of 12P/Pons-Brooks corroborates these observations, suggesting that its photochemical behavior is consistent with that of other well-studied comets.

Finally, we identified the sodium D lines at 5890 Åand 5896 Å, which indicate the existence of dust particles in the coma (Hyland et al., 2019). The atomic oxygen line [OI] at 6300 Åmay be associated with the dissociation of H_2O, indicating the presence of water, or it could be a result of atmospheric contribution from skyglow, especially given the comet's low altitude during observation (Swings, 1965).

3.2. The Dynamics Simulation

Comet 12P has well-defined orbital parameters that can be extracted with the `rebound` library. Table 1 lists the osculating orbital elements, and Figure 1 shows a plot of its orbit.

We integrated the orbit of comet 12P over 10^5 years in Prograde and Retrograde simulations, monitoring close encounters with Venus, Earth, Mars, Jupiter, and Saturn, as illustrated in Figure 3. To assess the sensitivity of the integrations, we introduced small perturbations in the initial orbit, corresponding to the confidence interval provided by the JPL/Horizons database, as follows: instead of integrating a single particle, we included 1000 test particles to enrich our analysis. According to the data obtained in the simulation, the closest approach to Earth occurred in 1883, the year in which William Brooks observed it, at $\sim$ 0.77 AU, before that, in 1811 at $\sim$ 1.15 AU, close to the observation by Jean-Louis Pons. In relation to Jupiter, the closest approach occurred in 1596 at $\sim$ 4.24 AU.

Comets with orbital periods shorter than 200 years and perihelion distances (q) less than 1.3 AU are classified as Near-Earth Comets (NECs). Our simulation, which is consistent with the current understanding, indicates that this comet meets the NEC criteria. However, it does not pose a threat, since its Minimum Orbit Intersection Distance (MOID) — defined as the smallest possible distance between the osculating orbits of two bodies — is greater than 0.05 AU (see (Li et al., 2019), for more details), despite the nucleus being approximately 10 km in diameter (Ye et al., 2020). According to JPL/Horizons, comet 12P had an encounter with Saturn in July 1957 at a distance of 1.6157 AU, which was reproduced in our simulation.

As shown in Figure 4, the orbital parameters of the test clones inserted within the confidence region associated with the orbital elements of comet 12P show significant variations between $15 \times 10^3 < t < 20 \times 10^3$ years.

This scatter reflects the sensitivity of the comet's orbit to small perturbations in the initial conditions, indicating that even subtle variations within the uncertainty bounds can generate significantly different trajectories over time. In extreme cases, we observed ejection from the solar system, with eccentricities $e > 1$ (5.09% of the simulated particles).

This behavior is expected because of the chaotic nature of the object. For short periods, the variation in orbital parameters can be attributed mainly to the initial differences introduced; however, the amplification of these differences over time highlights the importance of carefully incorporating orbital uncertainties in studies that require predictive accuracy. For 12P, the accuracy of

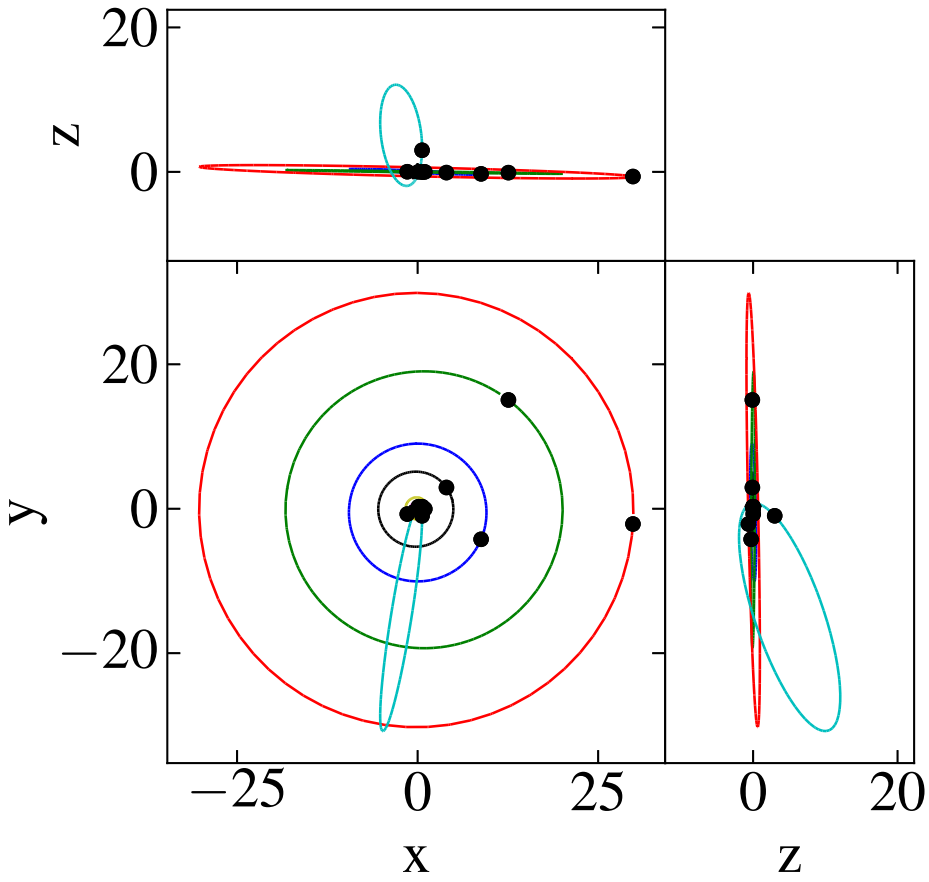

Figure 2. Three-dimensional representation of the orbit of comet 12P/Pons-Brooks and the planets Mercury through Neptune. The orbital elements were extracted from NASA Horizons using the `rebound` library.

the predictions is limited to time periods shorter than 20 thousand years.

3.3. Lyapunov Time and Orbital Chaos

To quantitatively assess the stability of comet 12P's orbit, we computed its maximum Lyapunov exponent, γ. The inverse of this exponent provides the Lyapunov time ($T_L = 1/\gamma$), which represents the characteristic timescale for two initially close trajectories to diverge exponentially, setting a horizon for the system's predictability. A positive and stable Lyapunov exponent is a definitive indicator of chaotic behavior.

For this analysis, we used the `REBOUND` package. We implemented the shadow particle method by creating a reference simulation that included the Sun, eight planets, and several dwarf planets, in three additional simulations. In each of these, the initial position of comet 12P was slightly perturbed by a small displacement $\epsilon = 10^{-8}$ AU along one of the Cartesian axes (x, y, and z). All four simulations were integrated in parallel using a high-precision IAS15 integrator. Throughout the integration, we measured the divergence between the reference orbit and each shadow orbit and calculated the Lyapunov exponent over time. The divergence vector was renormalized at each step to maintain numerical stability, following a procedure analogous to the Gram-Schmidt method.

The results of our calculations are shown in Figure 5. The Lyapunov exponents for all three perturbation directions converged to a stable positive value of $\gamma \approx 0.53$, unequivocally confirming the chaotic nature of comet 12P's orbit. This result is in excellent agreement with the findings of Królikowska et al. (2025), whose study classified 12P as dynamically unstable, on a time scale of 10^5 yr, they found a Lyapunov time of 297 ± 86 yr, which is in excellent agreement with our determination.

To estimate the Lyapunov time, we computed the inverse of the mean value of the Lyapunov exponent in the γ_x component. This results in $T_L = \frac{1}{0.351} \times 71.3 \approx 203.1$ yr. This indicates that the chaotic behavior of comet 12P manifests over a timescale of approximately 200 years. In other words, small perturbations in the initial conditions of comet 12P lead to an exponential divergence of trajectories after approximately 200 years. This is consistent with highly chaotic dynamical behavior, considering that chaoticity manifests itself in less than three orbital periods of the comet, as typically observed in trans-Neptunian objects and comets that interact gravitationally with giant planets.

Interestingly, our results can be contrasted with those of Emelyanenko (1985), who proposed that the 1:6 mean motion resonance with Jupiter could act as a temporary protective mechanism for the comet. Although resonances can offer short-term stability, our Lyapunov analysis demonstrates that the underlying dynamics of 12P are fundamentally chaotic. It is worth mentioning that chaos on short time scales does not necessarily imply large-scale changes in the orbit (see Milani & Nobili, 1992).

Furthermore, the decomposition of the exponents (right panel of Figure 5) reveals that the non-radial components ($\gamma_{\text{non-rad}}$) are

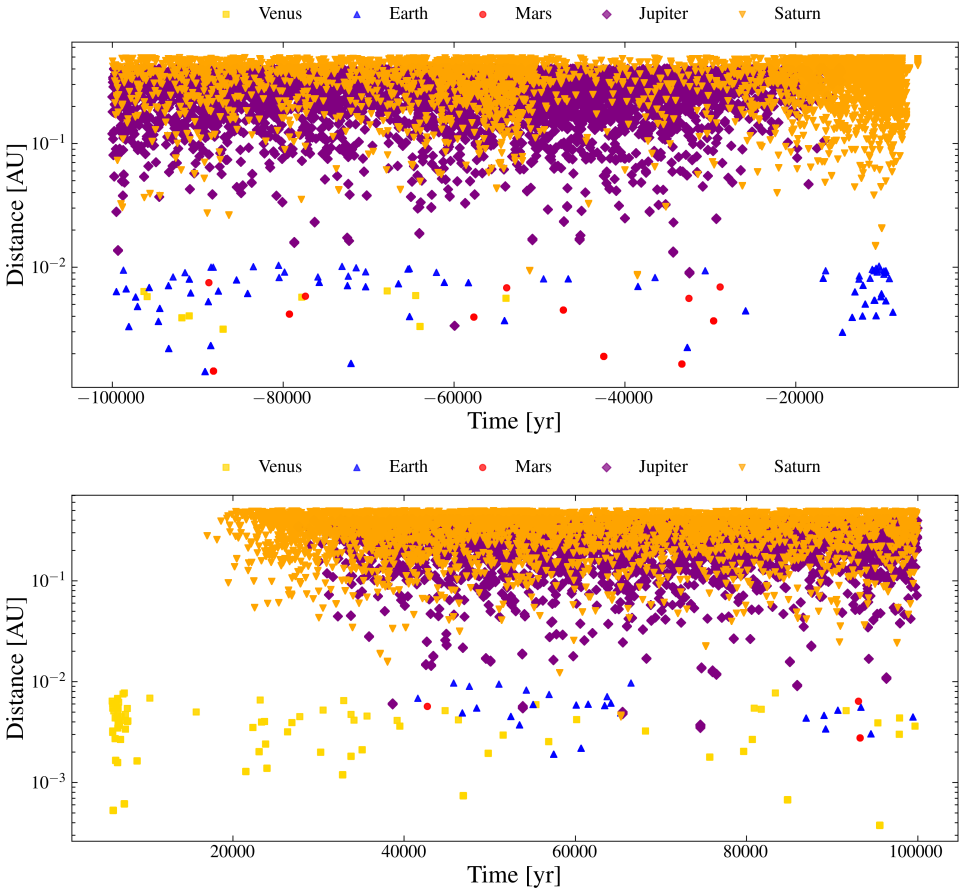

Figure 3. Close encounters recorded for 10^5 years in the past (top) and 10^5 year in the future (bottom) year between comet 12P and Venus (yellow squares), Earth (blue triangles), Mars (red circles), Jupiter (purple diamonds), and Saturn (yellow triangles). The rarity of close encounters between ∼10,000 years in the past and ∼20,000 years in the future suggests that the orbit is exceptionally stable during this period.

generally larger than the radial components ($\gamma_{\rm rad}$). This indicates that chaos primarily manifests as changes in the orientation of the orbit (i.e., its inclination and longitude of the ascending node) rather than significant changes in its shape (eccentricity and semi-major axis). This is a key physical insight, suggesting that the trajectory of a comet is more susceptible to tilting and twisting within the Solar System than to being directly ejected or radically changing its orbital energy on these timescales.

4. Discussion

Our dual approach, which combines a single-epoch spectroscopic snapshot near perihelion with a long-term dynamical analysis, provides a multifaceted view of comet 12P/Pons-Brooks.

4.1. Composition in the Context of an Active Comet

The detection of prominent emission bands of CN, C_2, NH_2, OI, and Na in our spectrum, obtained just 15 days before the perihelion, confirms that 12P/Pons-Brooks exhibits a typical cometary composition rich in carbon-chain molecules, as well as products of water and ammonia photodissociation. This finding aligns with the multi-epoch observations of Ferellec et al. (2024), who reported a typical C_2-rich composition in the months leading up to perihelion. Our work complements theirs by providing a snapshot during a period of maximum solar insolation, suggesting that the bulk composition of the outflowing gas remained relatively consistent throughout its inner Solar System passage.

However, the nature of 12P activity is far from quiescent. This comet is renowned for its dramatic outbursts, which release vast quantities of dust and gas. Jewitt & Luu (2025) characterized these outbursts as powerful events, likely driven by the crystallization of amorphous water ice, releasing kinetic energies on the order of 10^{14} J. In this context, our spectrum may sample not only the quiescent outflow but also the gas and dust freshly released during or shortly after such an outburst. The fact that the composition appears typical, in agreement with the pre-outburst phases observed by Ferellec et al. (2024), suggests that these energetic events primarily excavate and expel material from near-surface layers, which are compositionally similar to that sublimated during quiescent phases, rather than tapping into a chemically distinct primordial reservoir from the deep interior. Moreover, the challenges (Ferellec et al., 2024) faced in modeling the coma profiles with a standard Haser model, which pointed to the presence of extended sources or complex production pathways, are likely to be even more pronounced during the high-activity phase we observed. This highlights the difficulty of representing 12P's coma with standard models and the diagnostic value of spectra obtained during such transient, high-activity phases.

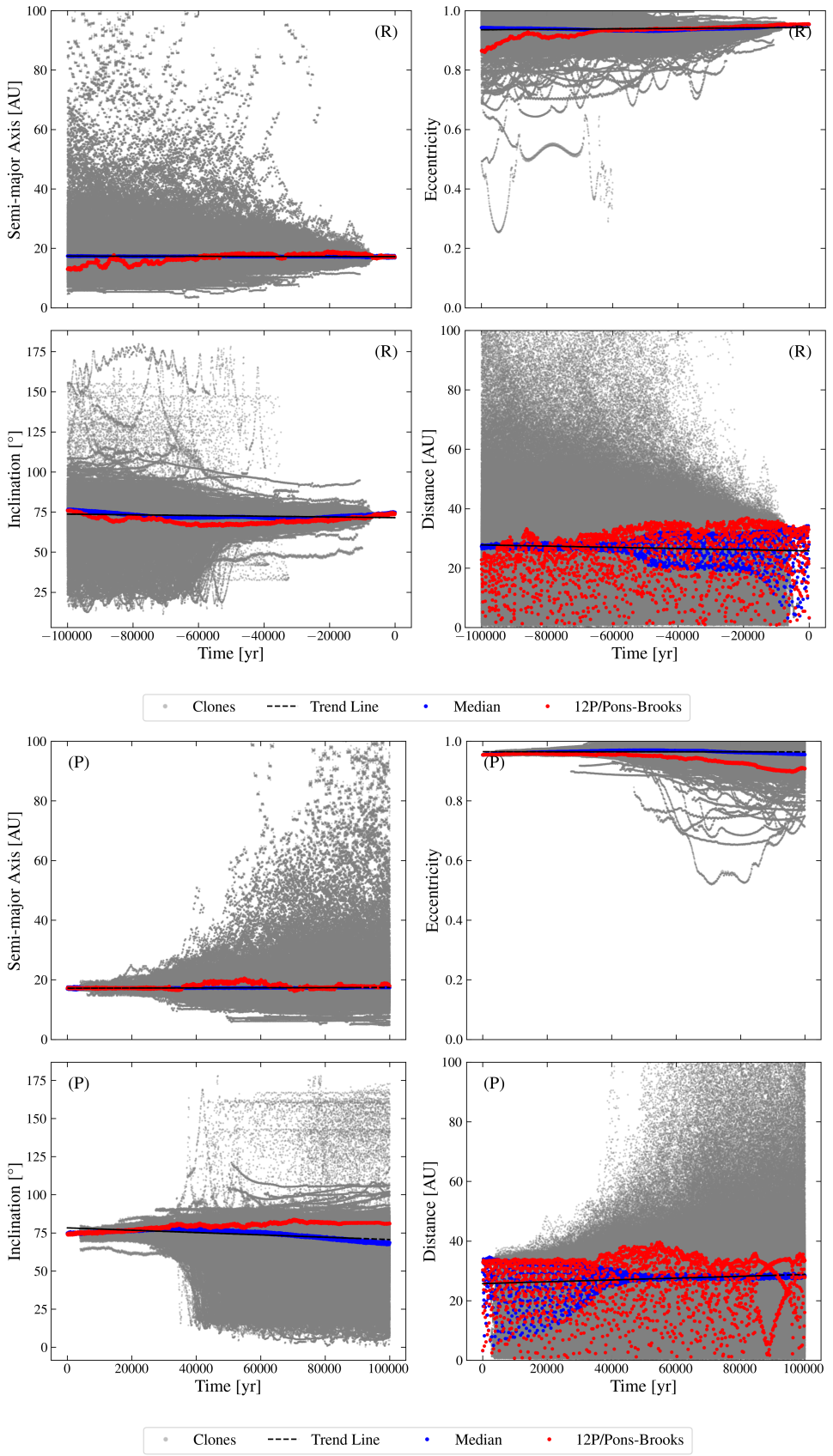

Figure 4. Evolution of orbital parameters recorded in Retrograde (top) and Prograde (bottom) simulations. The gray dots represent the Clones, the red dots represent the trajectory of comet 12P, the blue dots represent the Median, and the black line represents the Trend.

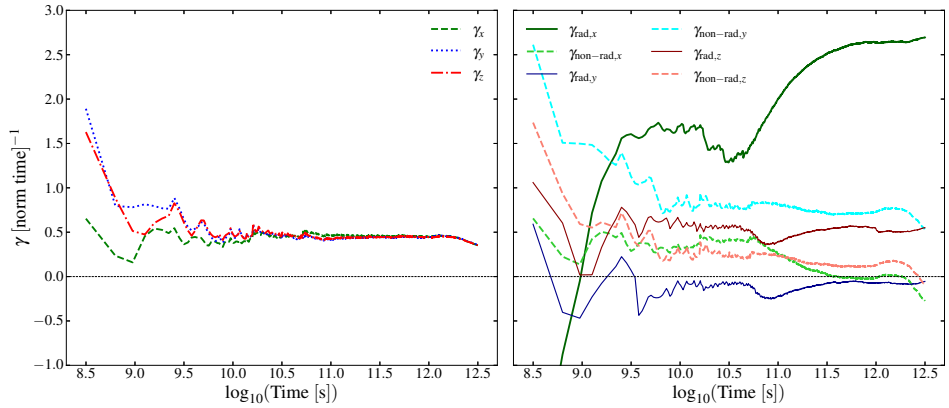

Figure 5. Evolution of the Lyapunov exponents (γ) for the orbit of comet 12P/Pons-Brooks over a simulation time of approximately 10^5 years. Left panel: Exponents calculated from the initial perturbations along the x (γ_x), y (γ_y), and z (γ_z) axes. Right Panel: Decomposition of these exponents into radial ($\gamma_{\rm rad}$) and non-radial ($\gamma_{\rm non\text{-}rad}$) components. The convergence of the exponents to a stable, positive value confirms the chaotic nature of the orbit.

4.2. Quantifying the Dynamical Chaos

Our dynamical analysis confirmed and quantified the chaotic nature of 12P's orbit. The dispersion of the 1000 test clones, which began to diverge significantly after 15—20 thousand years, is fully consistent with the findings of Meyer et al. (2020), who identified a similar timescale for the loss of orbital predictability in their backward integrations.

Crucially, our calculation of the Lyapunov time (T_L) provides a robust and quantitative measure of this instability. The resulting $T_L \approx 200$ years places 12P firmly in the category of dynamically unstable Halley-type comets, in strong agreement with the comprehensive survey by Królikowska et al. (2025). This short timescale for exponential divergence highlights the fundamental unpredictability of a comet's long-term path. While Emelyanenko (1985) suggested a protective 1:6 resonance with Jupiter, our Lyapunov analysis shows that any stabilizing effect from this resonance is ultimately overwhelmed by the underlying chaos driven by the cumulative planetary perturbations. Furthermore, the decomposition of the Lyapunov exponents revealed that chaos manifested more strongly in the non-radial components than in the radial components. This indicates that chaotic divergence is more likely to alter the inclination and nodal geometry than to lead to prompt ejection, producing a longer-lived but unpredictably oriented orbital path.

5. Conclusions

In this study, we conducted a dual-faceted study of the Halley-type comet 12P/Pons-Brooks, combining a single-epoch spectroscopic analysis near its 2024 perihelion with N-body simulations to assess its long-term dynamical stability. Our results provide a snapshot of the chemical composition of the comet during peak activity and quantitatively confirm the chaotic nature of its orbit.

The spectrum revealed prominent emission bands of CN, C_2, NH_2, Na, and [OI], consistent with a typical cometary composition rich in carbon chain molecules and the photodissociation products of water and ammonia. This is particularly significant, given the comet's powerful outbursts (Jewitt & Luu, 2025). Compared with the multi-epoch observations of Ferellec et al. (2024), our findings suggest that these events mainly excavate near-surface layers rather than exposing chemically distinct primordial reservoirs.

Our dynamical integrations further demonstrate 12P's strong orbital chaos. The divergence of 1000 orbital clones implies a predictability horizon of 15,000 – 20,000 years, consistent with Meyer et al. (2020), while the maximum Lyapunov exponent yields a Lyapunov time of $T_L \approx 200$ years, placing the comet among the most dynamically unstable Halley-type objects, in agreement with Królikowska et al. (2025). We conclude that any stabilizing influence of the proposed 1:6 resonance with Jupiter (Emelyanenko, 1985) is overwhelmed by cumulative planetary perturbations, with the dominant non-radial contributions indicating susceptibility to changes in orbital orientation rather than immediate ejection from the Solar System.

This study lays the groundwork for future research. Dedicated spectroscopic observations with facilities such as SOAR, especially in the violet region, would allow quantitative determination of OH and CN production rates, while continuum modeling could constrain dust properties and gas-to-dust ratios. Dynamically, the integrated orbital clone dataset produced here may be exploited in systematic searches for associated meteor showers (Christou, 2004; Tomko & Neslušan, 2016), offering new insights into the interplay between 12P's eruptive activity and its chaotic orbital evolution.

This research was supported by resources provided by the Scientific Computing Center (NCC/GridUNESP) and Orbital Dynamics and Planetology Group of the São Paulo State University (UNESP).

REFERENCES

Aravind, K., Venkataramani, K., Ganesh, S., Jehin, E., & Moulane, Y. 2024, JApA, 45, 11, doi: 10.1007/s12036-024-09996-6

Bockelée-Morvan, D., & Biver, N. 2017, RSPTA, 375, 20160252, doi: 10.1098/rsta.2016.0252

Bockelée-Morvan, D., Crovisier, J., Mumma, M. J., & Weaver, H. A. 2004, in Comets II, ed. M. C. Festou, H. U. Keller, & H. A. Weaver (Tucson: AZ, Univ. Arizona Press), 391

Cambianica, P., Munaretto, G., La Forgia, F., Fulle, M., & Cremonese, G. 2021, A&A, 656, A160, doi: 10.1051/0004-6361/202140309

Ceccarelli, C., Codella, C., Cabrit, S., Vastel, C., & Lefloch, B. 2022, arXiv e-prints, arXiv:2206.13270. https://arxiv.org/abs/2206.13270

Christou, A. A. 2004, Icar, 168, 23, doi: 10.1016/j.icarus.2003.12.006
Cochran, A. L., Barker, E. S., & Gray, C. L. 2012, Icar, 218, 144, doi: 10.1016/j.icarus.2011.12.010
Cochran, A. L., & Cochran, W. D. 2002, Icar, 157, 297, doi: 10.1006/icar.2002.6850
de Konkoly, N. 1884, MNRAS, 44, 251, doi: 10.1093/mnras/44.5.251
Emelyanenko, V. V. 1985, Soviet Astronomy Latters, II, 388
Evangelista-Santana, M. 2022, PhD thesis, About the nature of the Hyperbolic Comets, Observatório Nacional, Rio de Janeiro, Brazil
Feldman, P. D., Cochran, A. L., & Combi, M. R. 2004, in Comets II, ed. M. C. Festou, H. U. Keller, & H. A. Weaver (Tucson: Univ. Arizona Press), 425
Ferellec, L., Opitom, C., Donaldson, A., et al. 2024, MNRAS, 534, 1816, doi: 10.1093/mnras/stae2189
Gomes, R., Levison, H. F., Tsiganis, K., & Morbidelli, A. 2005, Natur, 435, 466, doi: 10.1038/nature03676
Hyland, M. G., Fitzsimmons, A., & Snodgrass, C. 2019, MNRAS, 484, 1347, doi: 10.1093/mnras/stz075
Irvine, W. M., Schloerb, F. P., Crovisier, J., Fegley, Bruce, J., & Mumma, M. J. 2000, in Protostars and Planets IV, ed. V. Mannings, A. P. Boss, & S. S. Russell (Tucson: Univ. Arizona Press), 1159
Jewitt, D., & Luu, J. 2025, AJ, 169, 338, doi: 10.3847/1538-3881/add2ff
Kawakita, H., & Watanabe, J.-i. 2002, ApJ, 572, L177, doi: 10.1086/341746
Kohoutek, L., & Rahe, J. 1976, in NASA Special Publication, ed. B. Donn, M. Mumma, W. Jackson, M. A'Hearn, & R. S. Harrington, Vol. 393, 159–181
Królikowska, M., Kankiewicz, P., & Wajer, P. 2025, MNRAS, 539, 590, doi: 10.1093/mnras/staf492
Li, M., Huang, Y., & Gong, S. 2019, Ap&SS, 364, 78, doi: 10.1007/s10509-019-3557-5
Meyer, M., Kobayashi, T., Nakano, S., Old, T., & Buzzi, L. 2020, arXiv:2012.15583, doi: 10.48550/arXiv.2012.15583
Milani, A., & Nobili, A. M. 1992, Natur, 357, 569, doi: 10.1038/357569a0
Mumma, M. J., & Charnley, S. B. 2011, ARA&A, 49, 471, doi: 10.1146/annurev-astro-081309-130811
Mumma, M. J., Weissman, P. R., & Stern, S. A. 1993, in Protostars and Planets III, ed. E. H. Levy & J. I. Lunine (Tucson: Univ. Arizona Press), 1177, doi: 1993prpl.conf.1177M
Munaretto, G., Cambianica, P., Cremonese, G., et al. 2023, P&SS, 230, 105664, doi: https://doi.org/10.1016/j.pss.2023.105664
Mura, A. 2023, Master's thesis, A decade of cometary spectroscopy from the Asiago 1.22 m telescope, Università degli Studi di Padova
Mura, A. C., La Forgia, F., Lazzarin, M., Farina, A., & Ochner, P. 2024, in EPSC 17, 1247, doi: 10.5194/epsc2024-1247
Newburn, R. L., J., & Yeomans, D. K. 1982, AREPS, 10, 297, doi: 10.1146/annurev.ea.10.050182.001501
Oates, J. C. T. 1986, Cambridge University Library: A History (Cambridge: MA, Cambridge Univ. Press)
Opitom, C., Jehin, E., Moulane, Y., Fitzsimmons, A., & Snodgrass, C. 2021, A&A, 650, L19, doi: 10.1051/0004-6361/202141245
Raymond, S. N., & Izidoro, A. 2017, Icar, 297, 134, doi: 10.1016/j.icarus.2017.06.030
Rein, H., & Liu, S. F. 2012, A&A, 537, A128, doi: 10.1051/0004-6361/201118085
Rein, H., & Spiegel, D. S. 2015, MNRAS, 446, 1424, doi: 10.1093/mnras/stu2164
Sagan, C., & Druyan, A. 2011, Comet (New York: NY, Ballantine Books)
Schechner, S. 1999, Comets, Popular Culture, and the Birth of Modern Cosmology (Princeton: NJ. Princeton Univ. Press)
Swings, P. 1965, QJRAS, 6, 28
Tomko, D., & Neslušan, L. 2016, A&A, 592, A107, doi: 10.1051/0004-6361/201628404
Walker, R. 2017, Select Spectral Atlas for Amateur Astronomers: A Guide to the Spectra of Astronomical Objects and Terrestrial Light Sources (Cambridge: MA, Cambridge University Press), doi: 10.1017/9781316694206
Walsh, K. J., Morbidelli, A., Raymond, S. N., O'Brien, D. P., & Mandell, A. M. 2011, Natur, 475, 206, doi: 10.1038/nature10201
Whipple, F. L. 1950, ApJ, 111, 375, doi: 10.1086/145272
Ye, Q., Farnham, T. L., Knight, M. M., Holt, C. E., & Feaga, L. M. 2020, RNAAS, 4, 101, doi: 10.3847/2515-5172/aba2d1
Yeomans, D. K. 1986, AJ, 91, 971, doi: 10.1086/114073